A PDE-ODE MODEL FOR A JUNCTION WITH RAMP BUFFER[*]

M. L. DELLE MONACHE[†], J. REILLY[‡], S. SAMARANAYAKE[‡], W. KRICHENE[‡],
P. GOATIN[§], AND A. M. BAYEN[‡]

Abstract. We consider the Lighthill–Whitham–Richards traffic flow model on a junction composed by one mainline, an onramp, and an offramp, which are connected by a node. The onramp dynamics is modeled using an ordinary differential equation describing the evolution of the queue length. The definition of the solution of the Riemann problem at the junction is based on an optimization problem and the use of a right-of-way parameter. The numerical approximation is carried out using a Godunov scheme, modified to take into account the effects of the onramp buffer. We present the result of some simulations and numerically check the convergence of the method.

Key words. scalar conservation laws, PDE-ODE systems, Riemann problem, macroscopic traffic flow models

AMS subject classifications. 90B20, 35L65

DOI. 10.1137/130908993

1. Introduction. Hydrodynamic models have commonly been used in the literature to describe the macroscopic evolution of vehicular traffic on roads and have been successfully generalized to networks in recent years. In the 1950s, Lighthill and Whitham [22] and Richards [25], independently, proposed a fluid dynamic model for traffic flow on an infinite single road, using a nonlinear hyperbolic partial differential equation (PDE). The Cauchy problem has successfully been extended to an initial-boundary value problem in [1] and then developed specifically for scalar conservation laws with concave flux in [19] and for traffic applications in [26]. More recently, several authors proposed models on networks that take into account different types of solutions at the intersections; see [5, 6, 9, 10, 13, 14, 15, 16] and the references therein.

In this article, we focus on a junction model designed for a ramp metering problem. Ramp metering models have been introduced in the engineering community in a discrete setting; see [23, 24] for details. In this article, we apply a continuous approach. We consider the scalar Lighthill–Whitham–Richards (LWR) model on a network composed of a single junction connecting a mainline, an onramp, and an offramp. The mainline evolution is described by a scalar conservation law, while the onramp dynamics is modeled by a buffer of infinite capacity, which is defined by an ordinary differential equation (ODE) depending on the difference between the incoming and outgoing fluxes at the ramp.

In the following sections, we prove the existence and uniqueness of solutions of the Riemann problem at the junction. The results are obtained by solving a linear

---

[†]Corresponding author. Inria Sophia Antipolis - Méditerranée, Sophia Antipolis, France 06902 (maria-laura.delle_monache@inria.fr).

[‡]Department of Civil and Environmental Engineering, University of California, Berkeley, Berkeley, CA 94720 (jackdreilly@berkeley.edu, samitha@gmail.com, walid@berkeley.edu, bayen@berkeley.edu).

[§]Inria Sophia Antipolis - Méditerranée, Sophia Antipolis France, 06902 (paola.goatin@inria.fr).

22

programming (LP) optimization problem. Unlike [11], where the flux through the junction is maximized, our LP-optimization consists of maximizing the flux on the outgoing mainline; see Remark 3 below. The offramp is treated as a sink, and a priority parameter is introduced to ensure uniqueness of the solution. As a modeling choice, the priority is satisfied in an approximate way, i.e., the priority will not always be respected, in benefit of flux maximization.

The article presents numerical approximations of possibly discontinuous solutions obtained using this model. In particular, we suitably modify the Godunov scheme to include the boundary conditions at the junction, as in [3, 7], and the ODE describing the buffer. This allows one to take into account the possible creation of an additional shock when the buffer empties. The scheme provides accurate numerical approximations, as shown by the numerical tests provided here.

The article is organized as follows. Section 2 contains some preliminary notation and definitions, while section 3 describes in detail the solution of the Riemann problem at the junction. In section 4 we introduce the numerical scheme with the particular boundary conditions used to compute approximate solutions to the problem. In section 5 we present some numerical tests which show the effectiveness of our approximation. Throughout the paper, we refer to [2, 8] for the general theory of hyperbolic conservation laws, and to [20, 21] for an introduction to the main numerical concepts.

2. Fundamental definitions and notation. We consider a junction with one mainline I modeled by the real line $]-\infty, +\infty[$, one onramp R_1, and one offramp R_2 at $x = 0$, as illustrated in Figure 1.
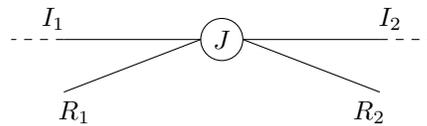

FIG. 1. *Junction modeled in the article.*

Note that Figure 1 is given for illustration purposes only; in particular, no assumptions are made on the spatial configuration of the ramps; i.e., we do not assume a particular order of the ramps. We also observe that, in the context of a network with multiple junctions, the model allows for junctions with no offramp (this can be achieved by setting the split ratio to zero) and junctions with no onramp (by setting the ramp demand to zero). From a macroscopic point of view, this means that on each mainline segment $I_1 =]-\infty, 0[$ and $I_2 =]0, +\infty[$, we consider the mass conservation equation

$$(2.1) \qquad \partial_t \rho + \partial_x f(\rho) = 0, \quad (t, x) \in \mathbb{R}^+ \times I_i,$$

where $\rho = \rho(t, x) \in [0, \rho_{\max}]$ is the mean traffic density, $\rho_{\max}$ is the maximal density allowed on the road, and the flux function $f : [0, \rho_{\max}] \to \mathbb{R}^+$ is given by the following flux-density relation:

$$f(\rho) = \rho v(\rho),$$

where $v(\rho)$ is a smooth decreasing function denoting the mean traffic speed.

Throughout the article, we assume for simplicity that the following hold:

(A1) $\rho_{\max} = 1$;
(A2) $f(0) = f(1) = 0$;
(A3) f is a strictly concave function.

Assumptions (A2) and (A3) ensure the existence and uniqueness of a maximum point of the flux function $\rho^{\mathrm{cr}} \in [0, 1]$. A typical example of a flux function for the LWR model is given in Figure 2.
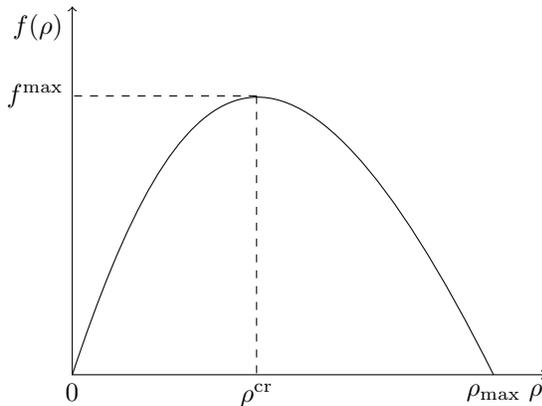

FIG. 2. *Flux function of* (2.1), *commonly referred to as a fundamental diagram in the transportation literature.*

On the onramp R_1 we consider the presence of a buffer modeled by the following ODE:

$$(2.2) \qquad \frac{dl(t)}{dt} = F_{\mathrm{in}}(t) - \gamma_{\mathrm{r1}}(t), \quad t \in \mathbb{R}^+,$$

where $l(t) \in [0, +\infty[$ is the length of the queue, $F_{\mathrm{in}}(t)$ is the flux that enters the onramp, and $\gamma_{\mathrm{r1}}(t)$ is the flux that exits from the onramp.

This particular choice is taken to avoid backward waves on the onramp boundary, which happens in the case of horizontal queues that consider vehicles arranged over the length of the roadway. In particular, at the left boundary of the onramp, backward-moving shock waves can result in lost information on the flux that actually enters the buffer. The presence of the buffer, considered as a vertical queue in which vehicles are stacked one upon the other, helps account for all the flow that enters the onramp; for details see [17]. For simplicity, we consider the offramp as a sink of infinite capacity that accepts all the flux entering from the mainline I_1, and we assume that no flux from the onramp is allowed in the offramp.

The Cauchy problem to solve is then

$$(2.3) \qquad \begin{cases} \partial_t \rho_i + \partial_x f(\rho_i) = 0, & (t, x) \in \mathbb{R}^+ \times I_i, \ i = 1, 2, \\ \dfrac{dl(t)}{dt} = F_{\mathrm{in}}(t) - \gamma_{\mathrm{r1}}(t), & t \in \mathbb{R}^+, \\ \rho_i(0, x) = \rho_{i,0}(x), & \text{on } I_i \ i = 1, 2, \\ l(0) = l_0, \end{cases}$$

where $\rho_i(0, x)$ represents the initial condition and $l_0 \in [0, +\infty[$ is the initial load of the buffer.

This will be coupled with an optimization problem at the junction which will give the distribution of the traffic among the roads.

We define the demand $d(F_{\text{in}}, l)$ of the onramp, the demand function $\delta(\rho_1)$ on the incoming mainline segment corresponding to the density ρ_1, and the supply function $\sigma(\rho_2)$ on the outgoing mainline segment corresponding to the density ρ_2 as follows:

$$(2.4) \qquad d(F_{\text{in}}, l) = \begin{cases} \gamma_{\text{r1}}^{\max} & \text{if } l(t) > 0, \\ \min\left(F_{\text{in}}(t), \gamma_{\text{r1}}^{\max}\right) & \text{if } l(t) = 0, \end{cases}$$

$$(2.5) \qquad \delta(\rho_1) = \begin{cases} f(\rho_1) & \text{if } 0 \leq \rho_1 < \rho^{\text{cr}}, \\ f^{\max} & \text{if } \rho^{\text{cr}} \leq \rho_1 \leq 1, \end{cases}$$

$$(2.6) \qquad \sigma(\rho_2) = \begin{cases} f^{\max} & \text{if } 0 \leq \rho_2 \leq \rho^{\text{cr}}, \\ f(\rho_2) & \text{if } \rho^{\text{cr}} < \rho_2 \leq 1, \end{cases}$$

where $\gamma_{\text{r1}}^{\max}$ is the maximal flow on the onramp and $f^{\max} = f(\rho^{\text{cr}})$ is the maximal flux on I_1 and I_2. Moreover, we introduce $\beta \in [0, 1]$, the split ratio of the offramp, and $\gamma_{\text{r2}}(t) = \beta f(\rho_1(t, 0-))$, its flux.

DEFINITION 2.1. *A triple $(\rho_1, \rho_2, l) \in \prod_{i=1}^{2} \mathcal{C}^0\left(\mathbb{R}^+; \mathbf{L}^1 \cap BV(\mathbb{R})\right) \times \mathbf{W}^{1,\infty}(\mathbb{R}^+; \mathbb{R}^+)$ is an admissible solution to (2.3) if the following hold:*

(i) *ρ_1, ρ_2 are weak solutions on I_1, I_2; i.e., $\rho_i : [0, +\infty[\times I_i \to [0, 1]$, $i = 1, 2$, such that*

$$(2.7) \qquad \int_{\mathbb{R}^+} \int_{I_i} \left(\rho_i \partial_t \varphi_i + f(\rho_i) \partial_x \varphi_i\right) dx\, dt = 0, \quad i = 1, 2,$$

for every $\varphi_i \in \mathcal{C}_c^1(\mathbb{R}^+ \times I_i)$.

(ii) *ρ_i satisfies the Kružhkov entropy condition [18] on $(\mathbb{R}^+ \times I_i)$; i.e., for every $k \in [0, 1]$ and for all $\varphi_i \in \mathcal{C}_c^1(\mathbb{R} \times I_i)$, $t > 0$,*

$$\int_{\mathbb{R}^+} \int_{I_i} (|\rho_i - k| \partial_t \varphi_i + \text{sgn}(\rho_i - k)(f(\rho_i) - f(k)) \partial_x \varphi_i) dx\, dt$$

$$(2.8) \qquad\qquad + \int_{I_i} |\rho_{i,0} - k| \varphi_i(0, x) dx \geq 0, \quad i = 1, 2.$$

(iii) *$f(\rho_1(t, 0-)) + \gamma_{\text{r1}}(t) = f(\rho_2(t, 0+)) + \gamma_{\text{r2}}(t)$.*

(iv) *The flux of the outgoing mainline $f(\rho_2(t, 0+))$ is maximum, subject to*

$$(2.9) \quad f(\rho_2(t, 0+)) = \min\left((1-\beta)\delta(\rho_1(t, 0-)) + d(F_{\text{in}}(t), l(t)), \sigma(\rho_2(t, 0+))\right)$$

and (iii).

(v) *l is a solution of (2.2) for almost every $t \in \mathbb{R}^+$.*

Remark 1. A parameter P is introduced in the next section to ensure uniqueness of the solution. $P \in]0, 1[$ is a right-of-way parameter that defines the amount of flux that enters the outgoing road from the incoming mainline and from the onramp. In particular, $P f(\rho_2(t, 0+))$ is the flux allowed from the incoming mainline into the outgoing mainline, and $(1 - P) f(\rho_2(t, 0+))$ the flux from the onramp. The use of a priority parameter to regulate traffic at an intersection was introduced in [4].

3. Riemann problem at the junction. In this section, we construct step by step the Riemann solver at the junction. This will be the building block for constructing approximate Godunov scheme (or wave-front tracking) solutions to general Cauchy problems. We fix constants $\rho_{1,0}, \rho_{2,0} \in [0, 1]$, $l_0 \in [0, +\infty[$, $F_{\text{in}} \in]0, +\infty[$,

and a priority factor $P \in \,]0,1[$. The Riemann problem at J is the Cauchy problem (2.3), where the initial conditions are given by $\rho_{0,i}(x) \equiv \rho_{0,i}$ in I_i for $i = 1, 2$. We define the Riemann solver by means of a Riemann solver $\mathcal{RS}_{\bar{l}}$, which depends on the instantaneous load of the buffer $\bar{l}$. For each $\bar{l}$ the Riemann solver $\mathcal{RS}_{\bar{l}}$ is constructed in the following way:

1. define $\Gamma_1 = f(\rho_1(t, 0-))$, $\Gamma_2 = f(\rho_2(t, 0+))$, $\Gamma_{r1} = \gamma_{r1}(t)$;
2. consider the space (Γ_1, Γ_{r1}) and the sets $\mathcal{O}_1 = [0, \delta(\rho_1)]$, $\mathcal{O}_{r1} = [0, d(F_{in}, \bar{l})]$;
3. trace the lines $(1 - \beta)\Gamma_1 + \Gamma_{r1} = \Gamma_2$ and $\Gamma_1 = \frac{P}{1-P}\Gamma_{r1}$;
4. consider the region

$$(3.1) \qquad \Omega = \Big\{ (\Gamma_1, \Gamma_{r1}) \in \mathcal{O}_1 \times \mathcal{O}_{r1} : (1 - \beta)\Gamma_1 + \Gamma_{r1} \in [0, \Gamma_2] \Big\}.$$

Different situations can occur depending on the value of Γ_2:

(i) Demand-limited case: $\Gamma_2 = (1 - \beta)\delta(\rho_1(t, 0-)) + d(F_{in}, \bar{l})$. We set Q to be the point $(\hat{\Gamma}_1, \hat{\Gamma}_{r1})$ such that $\hat{\Gamma}_1 = \delta(\rho_1(t, 0-))$, $\hat{\Gamma}_{r1} = d(F_{in}, \bar{l})$, and $\hat{\Gamma}_2 = (1 - \beta)\delta(\rho_1(t, 0-)) + d(F_{in}, \bar{l})$, as illustrated in Figure 3(a).
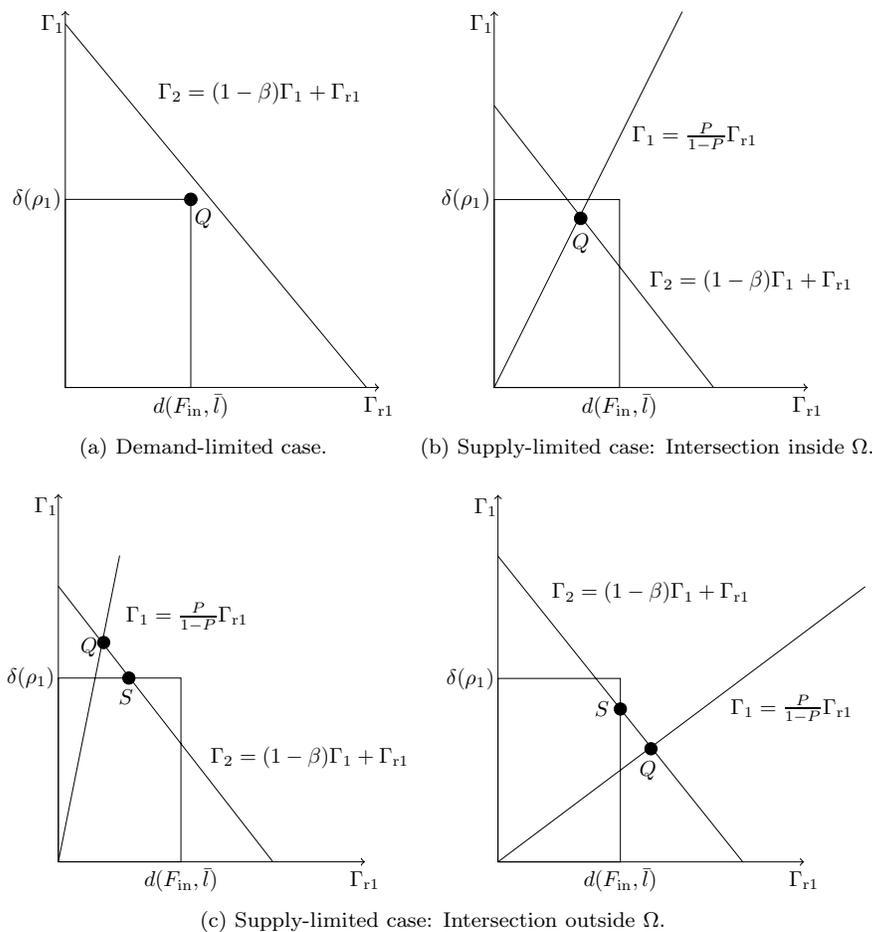

(a) Demand-limited case.   (b) Supply-limited case: Intersection inside Ω.

(c) Supply-limited case: Intersection outside Ω.

Fig. 3. *Solutions of the Riemann solver at the junction.*

(ii) Supply-limited case: $\Gamma_2 = \sigma(\rho_2(t, 0+))$. We set Q to be the point of intersection of $(1 - \beta)\Gamma_1 + \Gamma_{r1} = \Gamma_2$ and $\Gamma_1 = \frac{P}{1-P}\Gamma_{r1}$. If $Q \in \Omega$, we set $(\hat{\Gamma}_1, \hat{\Gamma}_{r1}) = Q$ and $\hat{\Gamma}_2 = \Gamma_2$; see Figure 3(b). If $Q \notin \Omega$, we set $(\hat{\Gamma}_1, \hat{\Gamma}_{r1}) = S$ and $\hat{\Gamma}_2 = \Gamma_2$, where S is the point of the segment $\Omega \cap (\Gamma_1, \Gamma_{r1}) : (1 - \beta)\Gamma_1 + \Gamma_{r1} = \Gamma_2$ closest to the line $\Gamma_1 = \frac{P}{1-P}\Gamma_{r1}$, obtained by solving the problem

$$
\begin{aligned}
\text{minimize} \quad & \left\| \begin{pmatrix} \gamma_{r1}(t) \\ f(\rho_1(t, 0-)) \end{pmatrix} - \left[\begin{pmatrix} \gamma_{r1}(t) \\ f(\rho_1(t, 0-)) \end{pmatrix} \cdot \alpha^P \right] \alpha^P \right\|_2^2 \\
\text{(3.2)} \qquad \text{subject to} \quad & f(\rho_2(t, 0+)) = (1 - \beta)f(\rho_1(t, 0-)) + \gamma_{r1}(t), \\
& \gamma_{r1}(t) \le d(F_{\text{in}}, \bar{l}), \\
& f(\rho_1(t, 0+)) \le \delta(\rho_1),
\end{aligned}
$$

where α^P is the normalized vector $\alpha^P = \frac{1}{\sqrt{P^2 + (1-P)^2}}\left(\begin{smallmatrix} P \\ 1-P \end{smallmatrix}\right)$; see Figure 3(c).

As can be seen in Figure 3(c), it might not be possible to respect the priority given by the parameter P if we also want to maximize the flux.

Once we have determined $\hat{\Gamma}_1$ and $\hat{\Gamma}_2$, we can define $\hat{\rho}_1$, $\hat{\rho}_2$ in a unique way as follows. We recall that $\rho = \rho^{\text{cr}} \in]0, 1[$ is the unique maximum point of the flux, and we define the function τ as follows; for details see [11].

DEFINITION 3.1. *Let $\tau : [0, 1] \to [0, 1]$ be the map such that the following hold:*
   (i) *$f(\tau(\rho)) = f(\rho)$ for every $\rho \in [0, 1]$;*
   (ii) *$\tau(\rho) \ne \rho$ for every $\rho \in [0, 1] \setminus \{\rho^{\text{cr}}\}$.*
Given

$$
\rho_1(0, \cdot) \equiv \rho_{1,0}, \qquad \rho_2(0, \cdot) \equiv \rho_{2,0},
$$

there exists a unique pair $(\hat{\rho}_1, \hat{\rho}_2) \in [0, 1]^2$ such that

$$
\text{(3.3)} \qquad \hat{\rho}_1 \in \begin{cases} \{\rho_{1,0}\} \cup]\tau(\rho_{1,0}), 1] & \text{if } 0 \le \rho_{1,0} \le \rho^{\text{cr}}, \\ [\rho^{\text{cr}}, 1] & \text{if } \rho^{\text{cr}} \le \rho_{1,0} \le 1, \end{cases} \qquad f(\hat{\rho}_1) = \hat{\Gamma}_1,
$$

and

$$
\text{(3.4)} \qquad \hat{\rho}_2 \in \begin{cases} [0, \rho^{\text{cr}}] & \text{if } 0 \le \rho_{2,0} \le \rho^{\text{cr}}, \\ \{\rho_{2,0}\} \cup [0, \tau(\rho_{2,0})[& \text{if } \rho^{\text{cr}} \le \rho_{1,0} \le 1, \end{cases} \qquad f(\hat{\rho}_2) = \hat{\Gamma}_2.
$$

For the incoming road the solution is given by the wave $(\rho_{1,0}, \hat{\rho}_1)$, while for the outgoing road the solution is given by the wave $(\hat{\rho}_2, \rho_{2,0})$. In this setting, given any initial data $\rho_{1,0}$, $\rho_{2,0}$, we can define $\mathcal{RS}_{\bar{l}} : [0, 1]^2 \to [0, 1]^2$ by

$$
\text{(3.5)} \qquad \mathcal{RS}_{\bar{l}}(\rho_{1,0}, \rho_{2,0}) = (\hat{\rho}_1, \hat{\rho}_2).
$$

Now given the initial load of the buffer $l_0 = \bar{l}$, the function $l(t)$ at time $t > 0$ is given according to the following possibilities, determined by straight integration of (2.2):
   1. If $F_{\text{in}} < \hat{\Gamma}_{r1}$, then

$$
\text{(3.6)} \qquad l(t) = \begin{cases} l_0 + (F_{\text{in}} - \hat{\Gamma}_{r1})t & \text{if } 0 < t < \frac{l_0}{\hat{\Gamma}_{r1} - F_{\text{in}}}, \\ 0 & \text{if } t > \frac{l_0}{\hat{\Gamma}_{r1} - F_{\text{in}}}. \end{cases}
$$

   2. If $F_{\text{in}} \ge \hat{\Gamma}_{r1}$, then

$$
\text{(3.7)} \qquad l(t) = l_0 + (F_{\text{in}} - \hat{\Gamma}_{r1})t \quad \forall t > 0.
$$

Remark 2. The presence of the buffer can create waves when the buffer empties at time $\bar{t} = -l_0/(F_{\text{in}} - \hat{\Gamma}_{\text{r1}}) > 0$ (with new values of the densities $\bar{\rho}_1, \bar{\rho}_2$) if $F_{\text{in}} < \hat{\Gamma}_{\text{r1}}$; see Figure 4.
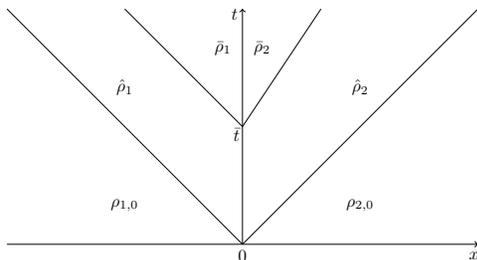

FIG. 4. *Solution of the Riemann problem.*

No waves are created instead if $F_{\text{in}} \geq \hat{\Gamma}_{\text{r1}}$, due to the infinite capacity of the buffer. Similar behavior is found in [13, 14] in a PDE-ODE model for supply chains. However, that model displays only waves with positive speeds, which suits supply chain behavior, and deals with a network which is mainly made up of 1×1 junctions where the queue is fed by the previous link and not by an external inflow. Moreover, when the network is extended to include also $m \times n$ junctions, the condition on the positivity of the speed ensures that boundary conditions are well defined without need for additional optimization problems at the nodes.

The following theorem ensures the consistency of $\mathcal{RS}_{\bar{l}}$.

THEOREM 3.2. *Consider a junction J and fix a priority parameter $P \in\,]0,1[$. For every $\rho_{1,0}, \rho_{2,0} \in [0,1]$ and $l_0 \in [0,+\infty[$ there exists a unique admissible solution $(\rho_1(t,x), \rho_2(t,x), l(t))$ compatible with the Riemann solver proposed in section 3, and the solution is given by*

$$(3.8) \qquad \rho_1(t,x) = \begin{cases} \rho_{1,0} & \text{if } x < \hat{s}_1 t, \\ \hat{\rho}_1 & \text{if } \hat{s}_1 t \leq x < \text{sgn}(\bar{t}^+) \cdot \min\left(0, \bar{s}_1(t-\bar{t})\right), \\ \bar{\rho}_1 & \text{if } \text{sgn}(\bar{t}^+) \cdot \min\left(0, \bar{s}_1(t-\bar{t})\right) \leq x < 0, \end{cases}$$

$$(3.9) \qquad \rho_2(t,x) = \begin{cases} \rho_{2,0} & \text{if } x \geq \hat{s}_2 t, \\ \hat{\rho}_2 & \text{if } \text{sgn}(\bar{t}^+) \cdot \max\left(0, \bar{s}_2(t-\bar{t})\right) \leq x < \hat{s}_2 t, \\ \bar{\rho}_2 & \text{if } 0 \leq x < \text{sgn}(\bar{t}^+) \cdot \max\left(0, \bar{s}_2(t-\bar{t})\right), \end{cases}$$

where $\hat{s}_1, \bar{s}_1, \hat{s}_2, \bar{s}_2$ are given by the Rankine–Hugoniot condition and $\bar{t} = -l_0/(F_{\text{in}} - \hat{\Gamma}_{\text{r1}})$. Moreover, for almost every $t > 0$, we have

$$(\rho_1(t,0-), \rho_2(t,0+)) = \mathcal{RS}_{l(t)}(\rho_1(t,0-), \rho_2(t,0+)).$$

In (3.8), (3.9), $\text{sgn}(\bar{t}^+) = 1$ if $\bar{t} > 0$; otherwise $\text{sgn}(\bar{t}^+) = 0$. The proof of the theorem is deferred until after some preliminary results. The mapping $\tau(\rho)$, as defined in (3.1), and the functions $\delta(\rho_1)$, $d(F_{\text{in}}, l)$, and $\sigma(\rho_2)$ yield the following properties.

LEMMA 3.3. *If $(\hat{\rho}_1, \hat{\rho}_2)$ is a solution of the Riemann problem with initial data $(\rho_{1,0}, \rho_{2,0})$, then the following holds:*

$$\delta(\rho_{1,0}) \leq \delta(\hat{\rho}_1),$$
$$\sigma(\rho_{2,0}) \leq \sigma(\hat{\rho}_2),$$
$$d(F_{\text{in}}, l_0) \leq d(F_{\text{in}}, l).$$

Proof. For the incoming road we have

$$\begin{aligned}
\delta(\rho_{1,0}) &\leq \delta(\hat{\rho}_1) \quad \text{if } 0 \leq \rho_{1,0} \leq \rho^{\text{cr}}, \\
\delta(\rho_{1,0}) &= \delta(\hat{\rho}_1) \quad \text{if } \rho^{\text{cr}} \leq \rho_{1,0} \leq 1.
\end{aligned}$$

(3.10)

In particular, if $\rho_{1,0} \in [0, \rho^{\text{cr}}]$, either $\hat{\rho}_1 \in \,]\tau(\rho_{1,0}), 1]$ or $\hat{\rho}_1 = \rho_{1,0}$. In the first case, $\delta(\rho_{1,0}) = f(\rho_{1,0}) \leq f^{\max} = \delta(\hat{\rho}_1)$ (see Figure 5(a)), while in the second case $\delta(\rho_{1,0}) = f(\rho_{1,0}) = f(\hat{\rho}_1) = \delta(\hat{\rho}_1)$ (see Figure 5(b)). On the other hand, if $\rho_{1,0} \in [\rho^{\text{cr}}, 1]$, then $\hat{\rho}_1 \in [\rho^{\text{cr}}, 1]$ and $\delta(\rho_{1,0}) = f^{\max} = \delta(\hat{\rho}_1)$ (see Figure 5(c)).

(a) $0 \leq \rho_{1,0} \leq \rho^{\text{cr}}$.   (b) $\rho_{1,0} = \hat{\rho}_1$.
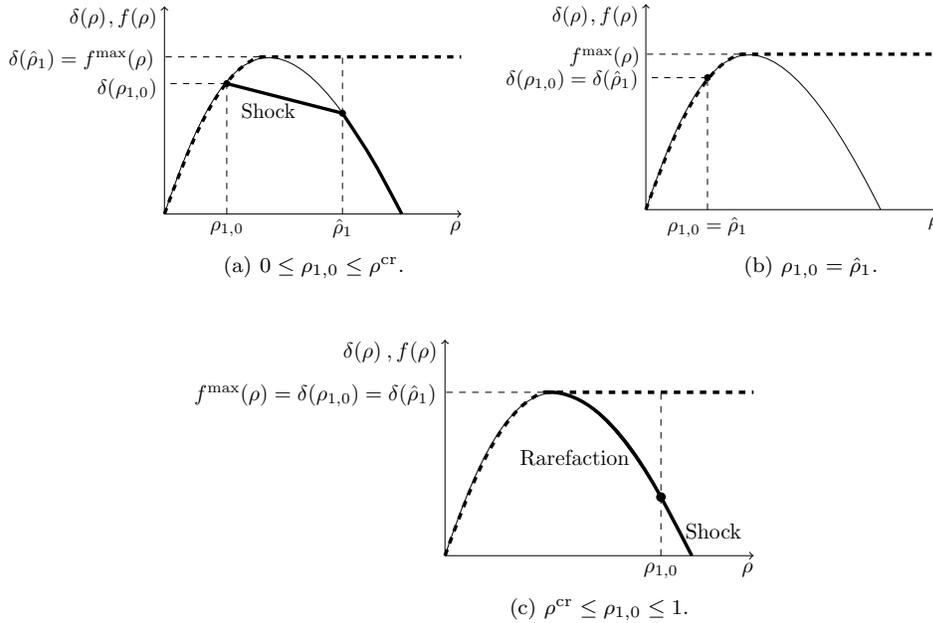
(c) $\rho^{\text{cr}} \leq \rho_{1,0} \leq 1$.

FIG. 5. *Instantaneous evolution of the demand in the Riemann problem (incoming road).*

Using the same approach for the outgoing road, we have

$$\begin{aligned}
\sigma(\rho_{2,0}) &= \sigma(\hat{\rho}_2) \quad \text{if } 0 \leq \rho_{2,0} \leq \rho^{\text{cr}}, \\
\sigma(\rho_{2,0}) &\leq \sigma(\hat{\rho}_2) \quad \text{if } \rho^{\text{cr}} \leq \rho_{2,0} \leq 1,
\end{aligned}$$

(3.11)

In particular, if $0 \leq \rho_{2,0} \leq \rho^{\text{cr}}$, then $0 \leq \hat{\rho}_2 \leq \rho^{\text{cr}}$ as well, and $\sigma(\rho_{2,0}) = f^{\max} = \sigma(\hat{\rho}_2)$; see Figure 6(c). Otherwise $\rho^{\text{cr}} \leq \rho_{2,0} \leq 1$, and either $\hat{\rho}_2 = \rho_{2,0}$ or $\hat{\rho}_2 \in [0, \tau(\rho_{2,0})[$. In the first case, $\sigma(\rho_{2,0}) = f(\rho_{2,0}) = f(\hat{\rho}_2) = \sigma(\hat{\rho}_2)$; see Figure 6(b). In the second case, $\sigma(\rho_{2,0}) = f(\rho_{2,0}) \leq f^{\max} = \sigma(\hat{\rho}_2)$; see Figure 6(a).

For the onramp, we consider two different cases, when the buffer is initially empty and when it is not. In both cases different situations can occur.

(L1) Initially empty buffer: $l(0) = 0 \Rightarrow d(F_{\text{in}}, l(0)) = \min(F_{\text{in}}, \gamma_{\text{r1}}^{\max})$.

(L1.1) Buffer increases: $l(0+) > 0 \Rightarrow d(F_{\text{in}}, l(0+)) = \gamma_{\text{r1}}^{\max}$. If $d(F_{\text{in}}, l(0)) = F_{\text{in}}$, then $d(F_{\text{in}}, l(0)) \leq d(F_{\text{in}}, l(0+))$. If $d(F_{\text{in}}, l(0)) = \gamma_{\text{r1}}^{\max}$, then $d(F_{\text{in}}, l(0)) = d(F_{\text{in}}, l(0+))$.

(L1.2) Buffer remains empty: $l(0+) = 0 \Rightarrow d(F_{\text{in}}, l(0+)) = \min(F_{\text{in}}, \gamma_{\text{r1}}^{\max})$. Hence, $d(F_{\text{in}}, l(0)) = d(F_{\text{in}}, l(0+))$.
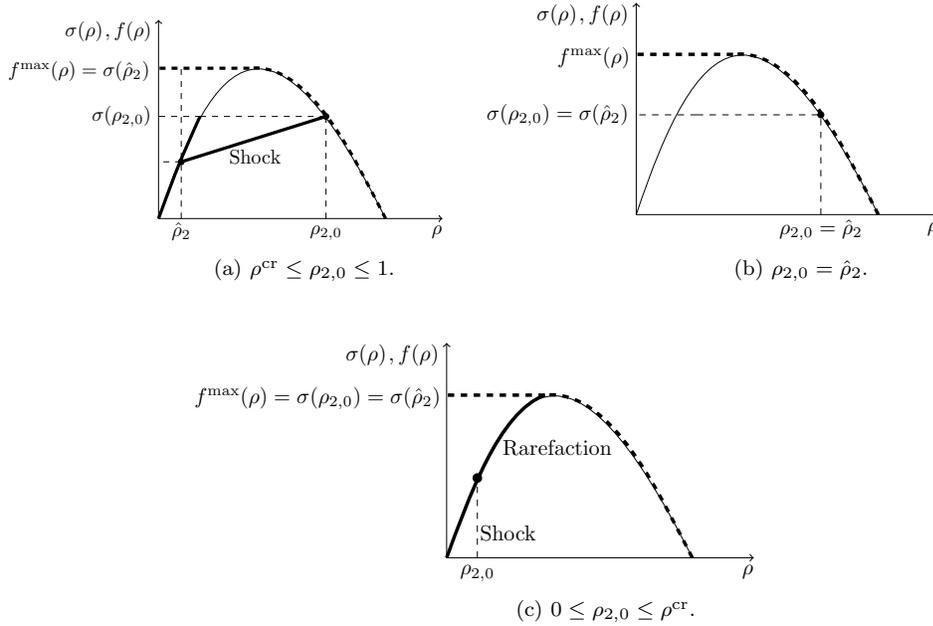
FIG. 6. *Instantaneous evolution of the supply in the Riemann problem (outgoing road).*

(L2) Buffer initially not empty: $l(0) > 0 \Rightarrow d(F_{\text{in}}, l(0)) = \gamma_{\text{r1}}^{\max}$.

(L2.1) Buffer grows (decreases) linearly: $0 < l(0) < l(0+)$ $(0 < l(0+) < l(0)) \Rightarrow$ $d(F_{\text{in}}, l(0+)) = \gamma_{\text{r1}}^{\max}$. Hence, $d(F_{\text{in}}, l(0)) = d(F_{\text{in}}, l(0+))$.
This concludes the proof.   □

Now we are ready to prove Theorem 3.2.

Proof of Theorem 3.2. Existence and uniqueness follow by construction of the Riemann solver detailed at the beginning of this section. In the following we will show the proof of the consistency of $\mathcal{RS}_{l(t)}$.

Fix $t_0 \geq 0$. If $(\rho_1(t_0, 0-), \rho_2(t_0, 0+))$ is a solution of the Riemann solver, corresponding to the same buffer value $l(t_0)$, we need to show that

$$\mathcal{RS}_{l(t_0)}(\rho_1(t_0, 0-), \rho_2(t_0, 0+)) = (\rho_1(t_0, 0-), \rho_2(t_0, 0+)).$$

Without loss of generality, we fix $t_0 = 0$, and we keep the same notation used in the proof of Lemma 3.3.

We show that the optimal point in the feasible set Ω, as defined in (3.1), resulting from the Riemann solver does not change. From the results of Lemma 3.3 it is straightforward to say that the set Ω either increases between times $t = 0$ and $t > 0$ or does not change; see Figures 7 and 8. Now, we need to prove that the optimal point does not change. We treat the supply-limited and the demand-limited cases separately.

1. Supply-constrained junction problem; see Figure 7. We assume that we are supply-limited at $t = 0$. In this case, by construction of the Riemann solver, it holds that $\rho_{2,0} = \hat{\rho}_2$ and hence $\sigma(\rho_{2,0}) = \sigma(\hat{\rho}_2)$. The priority line is fixed, and the point of intersection Q does not change.

(i) Optimal solution inside Ω; see Figure 7(a). Since Q is determined by the intersection of the two lines and Ω can only increase $(\delta(\rho_{1,0}) \leq \delta(\hat{\rho}_1), d(F_{\text{in}}, l(0)) \leq$

(a) $Q \in \Omega$.

(b) $Q \notin \Omega$, $\hat{\Gamma}_1 = \delta(\rho_{1,0})$.

(c) $Q \notin \Omega$, $\hat{\Gamma}_{r1}(0) = d(F_{\text{in}}, l_0)$.
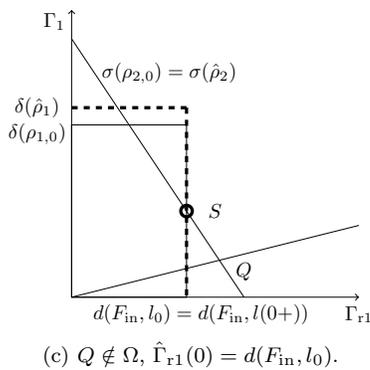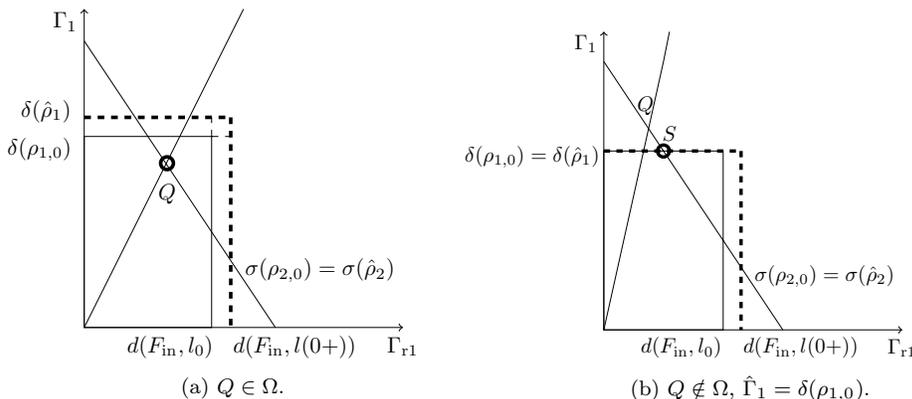
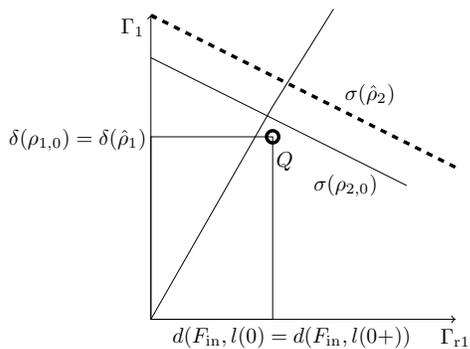Fig. 7. *Supply-constrained junction problems.*

Fig. 8. *Demand-constrained junction problem.*

$d(F_{\text{in}}, l(0+)))$, we have

$$(\hat{\rho}_1, \hat{\rho}_2) = \mathcal{RS}_{l(0)}(\hat{\rho}_1, \hat{\rho}_2).$$

(ii) Optimal solution on the border of Ω, $\hat{\Gamma}_1 = \delta(\rho_{1,0})$; see Figure 7(b). We have to prove that the result of the minimization problem (3.2) (the point S in the figure) does not change. In this case, by construction of the Riemann solver it holds that $\rho_{1,0} = \hat{\rho}_1$. This yields $\delta(\rho_{1,0}) = \delta(\hat{\rho}_1)$ by (3.10). Since, $d(F_{\text{in}}, l(0))$ can increase only

according to the cases (L1) and (L2), we have

$$(\hat{\rho}_1, \hat{\rho}_2) = \mathcal{RS}_{l(0)}(\hat{\rho}_1, \hat{\rho}_2).$$

(iii) Optimal solution on the border of Ω, $\hat{\Gamma}_{r1}(0) = d(F_{in}, l(0))$; see Figure 7(c). For the onramp, the only case where the demand can increase is the case (L1.1). In this particular setting, if $d(F_{in}, l(0)) = F_{in}$, it holds that $\gamma_{r1}(0) = F_{in}$ and $F_{in} \leq \gamma_{r1}^{max}$. When the buffer increases we have $\gamma_{r1}(0+) = d(F_{in}, l(0+)) = \gamma_{r1}^{max}$, which implies $\gamma_{r1}^{max} \leq F_{in}$. Hence, $F_{in} = \gamma_{r1}^{max}$ and $d(F_{in}, l(0)) = d(F_{in}, l(0+))$. The mainline demand can only increase. Hence,

$$(\hat{\rho}_1, \hat{\rho}_2) = \mathcal{RS}_{l(0)}(\hat{\rho}_1, \hat{\rho}_2).$$

2. Demand-constrained junction problem; see Figure 8. $\Omega = \Omega(\rho_{1,0}, l(0)) = \Omega(\hat{\rho}_1, l(0))$. In fact, $\rho_{1,0} = \hat{\rho}_1$, and for the onramp it holds that $\gamma_{r1}^{max} = F_{in}$ (as in the previous point), and this yields $\delta(\rho_{1,0}) = \delta(\hat{\rho}_1)$ and $d(F_{in}, l(0)) = d(F_{in}, l(0+))$ by (3.10) and (L1) and (L2). The supply can only increase, by (3.11). Hence,

$$(\hat{\rho}_1, \hat{\rho}_2) = \mathcal{RS}_{l(0)}(\hat{\rho}_1, \hat{\rho}_2).$$

Moreover, the limiting side of Ω does not change; i.e., it is not possible to pass from a demand-constrained junction problem to a supply-limited one and vice versa. This follows from the fact that $\sigma(\rho_{2,0}) = \sigma(\hat{\rho}_2)$ when we have a supply-limited junction problem (Figure 7), and $d(F_{in}, l(0)) = d(F_{in}, l(0+))$, $\delta(\rho_{1,0}) = \delta(\hat{\rho}_1)$ when we have a demand constrained junction problem (Figure 8).

This concludes the proof.   □

Remark 3. The proposed model is a variant of the junction model considered in [5] in the 2×2 case. In [5], the traffic distribution across the junction is given by a distribution matrix A, subject to technical conditions that ensure uniqueness of the solution. In our case, since we suppose that no flux from the onramp is directed into the offramp, the distribution matrix would look like: $A = \begin{pmatrix} 1-\beta & 1 \\ \beta & 0 \end{pmatrix}$. Clearly, as the offramp gets more congested, β decreases. If we solve the model proposed in [5] using this distribution matrix, there can be cases in which the solution gives zero onramp flux; see Figure 9(a). This is due to the choice to maximize the flow throughout the junction. In fact, in this way, the model tends to satisfy the mainline demand before the onramp one. This does not reflect what happens in reality, since the demand allocation depends on the number of lanes available for each inflow; for details, see [17]. Hence, we propose a model that fixes this issue of balancing the flux between the two incoming roads by the introduction of a right-of-way parameter. In particular, the priority coefficient keeps the maximization point far from the axis, avoiding blocking; see Figure 9(b).

Remark 4. This model extends the use of a priority parameter, as introduced in [4], to the case of 2×2 junctions. In [4], the authors use the priority parameter only for 2×1 junctions, treating 2×2 junctions with a traffic distribution matrix which can result, in our setting, in onramp blocking as explained in the previous remark.

4. Numerical approximation. In order to find approximate solutions, we adapt the classical Godunov scheme to the problem, with some adjustment due to the presence of the buffer.

We define a numerical grid in $(0, T) \times \mathbb{R}$ using the following notation:
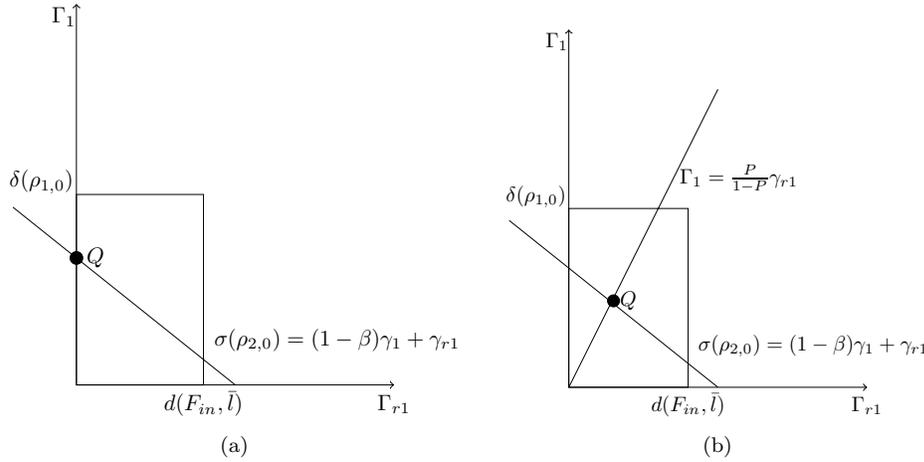
(i) Δx is the fixed space grid size;

FIG. 9. *Comparison between the Coclite–Garavello–Piccoli model* [5] (a) *and our model* (b).

(ii) Δt^n is the nonuniform time grid size given by the CFL condition;

(iii) $(t^n, x_j) = (t^{n-1} + \Delta t^n, j\Delta x)$ for $n \in \mathbb{N}$ and $j \in \mathbb{Z}$ are the grid points.

For a function v defined on the grid we write $v_j^n = v(t^n, x_j)$ for j, n varying on a subset of $\mathbb{Z}$ and $\mathbb{N}$, respectively. We also use the notation u_j^n for $u(t^n, x_j)$ when u is a continuous function on the (t, x) plane.

4.1. Godunov scheme. The Godunov scheme as introduced in [12] is based on exact solutions to Riemann problems. The main idea of this method is to approximate the initial datum by a piecewise constant function, then the corresponding Riemann problems are solved exactly, and a global solution is simply obtained by piecing them together. Finally, one takes the mean on the cell and proceeds by induction. Consider the hyperbolic problem with initial data

$$(4.1) \qquad \partial_t u + \partial_x f(u) = 0, \quad x \in \mathbb{R}, \ t \in [0, T],$$

$$(4.2) \qquad u(0, x) = u_0(x), \quad x \in \mathbb{R}.$$

A solution of the problem is constructed taking a piecewise constant approximation of the initial data,

$$(4.3) \qquad v_j^0 = \frac{1}{\Delta x} \int_{x_{j-1/2}}^{x_{j+1/2}} u_0(x)dx, \quad j \in \mathbb{Z},$$

and defining v_j^n recursively starting from v_j^0, as follows:

$$(4.4) \qquad v_j^{n+1} = \frac{1}{\Delta x} \int_{x_{j-1/2}}^{x_{j+1/2}} v^\Delta(t^{n+1}, x)dx.$$

Under the CFL condition

$$(4.5) \qquad \Delta t^n \max_{j \in \mathbb{Z}} \left| \lambda_{j+\frac{1}{2}}^n \right| \leq \frac{1}{2}\Delta x,$$

the waves generated by different Riemann problems do not interact. Above, $\lambda_{j+\frac{1}{2}}^n$ is the wave speed of the Riemann problem solution at the interface $x_{j+\frac{1}{2}}$ at time t^n. Under the condition (4.5) the scheme can be written as

$$(4.6) \qquad v_j^{n+1} = v_j^n - \frac{\Delta t^n}{\Delta x}(g(v_j^n, v_{j+1}^n) - g(v_{j-1}^n, v_j^n)),$$

where numerical flux g takes in general the following expression:

$$(4.7) \qquad g(u,v) = \left\{ \begin{array}{ll} \min_{z \in [u,v]} f(z) & \text{if } u \le v, \\ \max_{z \in [v,u]} f(z) & \text{if } v \le u. \end{array} \right.$$

4.2. Boundary conditions and conditions at the junctions. Here we impose the boundary conditions for the incoming and the outgoing roads at the endpoint not connected to the junction. We also assign boundary conditions at the endpoints of the roads connected to the junction. In both cases we will use the classical approach for road networks as introduced in [3].

Boundary conditions. Each road is divided into $J + 1$ cells numbered from 0 to J. For the incoming road, in practice, we proceed by defining

$$v_0^{n+1} = v_0^n - \frac{\Delta t^n}{\Delta x}(g(v_0^n, v_1^n) - f(v_0^n)),$$

where $f(v_0^n)$ is the value of the flux at the boundary.

An outgoing boundary can be treated analogously,

$$v_J^{n+1} = v_J^n - \frac{\Delta t^n}{\Delta x}(f(v_J^n) - g(v_{J-1}^n, v_J^n)),$$

with $f(v_J^n)$ the outgoing flux.

Since we are dealing with Riemann problems at the junction, the formulation of absorbing boundary conditions is equivalent to that with the ghost cells, which is common in literature; see, for details, [3, 5, 27].

Conditions at the junction. For I_1, which is connected at the junction at the right endpoint, we set

$$v_J^{n+1} = v_J^n - \frac{\Delta t^n}{\Delta x}(\hat{\Gamma}_1 - g(v_{J-1}^n, v_J^n)),$$

while for the outgoing road, connected at the junction at the left endpoint, we have

$$v_0^{n+1} = v_0^n - \frac{\Delta t^n}{\Delta x}(g(v_0^n, v_1^n) - \hat{\Gamma}_2),$$

where $\hat{\Gamma}_1$ and $\hat{\Gamma}_2$ are the maximized fluxes computed in section 3.

Remark 5. For the Godunov scheme there is no need to invert the flux f to compute the corresponding density in the scheme, as the Godunov flux coincides with the Riemann flux. In this case it suffices to insert the computed maximized fluxes directly into the scheme.
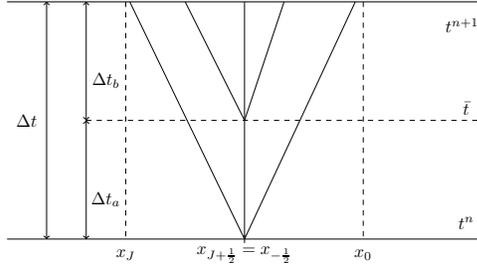
FIG. 10. *Junction in the case of an emptying buffer.*

4.3. ODE treatment. Let us consider now the buffer modeled by (2.2) on the onramp. At each time step $t^n = t^{n-1} + \Delta t^n$ we compute the new value of the queue length according to two possible cases, with Euler first order integration:

1. If $F_{in}(t^n) < \hat{\Gamma}_{r1}$,

$$l^{n+1} = \begin{cases} l^n + (F_{in}(t^n) - \hat{\Gamma}_{r1})\Delta t^n & \text{for } t^{n+1} < \bar{t}, \\ 0 & \text{otherwise.} \end{cases}$$

2. If $F_{in}(t^n) \geq \hat{\Gamma}_{r1}$,

$$l^{n+1} = l^n + (F_{in}(t^n) - \hat{\Gamma}_{r1})\Delta t^n.$$

Above, $\hat{\Gamma}_{r1}$ is the maximized flux described in section 3, $F_{in}(t^n)$ is the flux entering the onramp at t^n given by

$$F_{in}(t^n) = \frac{1}{\Delta t^n} \int_{t^n}^{t^{n+1}} F_{in}(t)dt,$$

and $\bar{t}$ is the time at which the buffer empties. We can calculate the time at which the buffer can empty for each time step Δt^n:

(4.8) $$\bar{t} = -\frac{l^n}{F_{in}(t^n) - \hat{\Gamma}_{r1}} + t^n.$$

4.4. Modified Godunov scheme. The Godunov scheme cannot be applied as it is when the buffer empties, as noted in [7], because the solution could potentially not be self-similar. If the buffer empties, at some time step Δt^n, we might have multiple shocks at the junction. In this case we divide the time step $\Delta t^n = (t^n, t^{n+1})$ into two subintervals $\Delta t_a = (t^n, \bar{t})$ and $\Delta t_b = (\bar{t}, t^{n+1})$, as in Figure 10, with $\bar{t}$ being defined in (4.8). Then, we solve in one time step two different Riemann problems at the junction. For Δt_a we solve the classical Godunov scheme. For the Δt_b we solve a new Riemann problem at the junction in which the value of the queue length is $l = 0$. The junction conditions are

(4.9) $$v_J^{n+1} = v_J^{\bar{t}} - \frac{\Delta t_b}{\Delta x}\left(\hat{\Gamma}_1^{\bar{t}} - g(v_{J-1}^n, v_J^{\bar{t}})\right),$$

(4.10) $$v_0^{n+1} = v_0^{\bar{t}} - \frac{\Delta t_b}{\Delta x}\left(g(v_0^{\bar{t}}, v_1^n) - \hat{\Gamma}_2^{\bar{t}}\right),$$

where with the superscript $\bar{t}$ we indicate the value computed at $t = \bar{t}$ in the previous time step Δt_a.

Remark 6. We point out that in our case it is not necessary to introduce an explicit correction on the ODE, as done in [7], since at time $\bar{t}$ we compute ex novo the Riemann problem at the junction with a queue length equal to zero.

5. Numerical results. For illustration, we choose a concave fundamental diagram with the following flux function:

$$f(\rho) = V_{\max}\rho(1 - \rho),$$

where $V_{\max}$ is the maximal velocity of the traffic flow. In this case the Godunov numerical flux is given by

$$(5.1) \qquad g(u, v) = \begin{cases} \min\left(f(u), f(v)\right) & \text{if } u \leq v, \\ f(u) & \text{if } v < u < \rho^{\mathrm{cr}}, \\ f^{\max} & \text{if } v < \rho^{\mathrm{cr}} < u, \\ f(v) & \text{if } \rho^{\mathrm{cr}} < v < u. \end{cases}$$

In this section we present some numerical tests performed with the scheme previously described. We introduce the formal order of convergence μ of a numerical method,

$$(5.2) \qquad \mu = \frac{\ln(\mathrm{TOT}_{\mathrm{err}})}{\ln(dx)},$$

where the $\mathbf{L}^1$-norm error is given by

$$(5.3) \qquad \mathrm{TOT}_{\mathrm{err}} = \sum_{i=1}^{2} \|u_e^i - u_c^i\|_{\mathbf{L}^1},$$

where u_e^i and u_c^i are the exact solution and the computed solution, respectively, in each road. We show some numerical results obtained by applying Godunov scheme to problem (2.3). Tables 1 and 2 provide the values of the $\mathbf{L}^1$-error (5.3) and the order of convergence (5.2). Here we deal with a mainline of length 8, parametrized by the interval $[-4, 4]$ with the node placed at $x = 0$, such that $I_1 = [-4, 0]$ and $I_2 = [0, 4.]$ In all the simulations we fix $V_{\max} = 1$, $P = 0.7$, $\beta = 0.2$, $\gamma_{\max} = 0.5$, $l_0 = 0.2$, and $F_{\mathrm{in}} = 0.05$.

1. *Case* I: We consider the following initial data:

$$(5.4) \qquad \rho_1(0, x) = 0.6, \quad \rho_2(0, x) = 0.$$

The values of the initial conditions create a shock on the incoming mainline and a rarefaction on the outgoing one. After a time $t = 5.3$ we can see the rarefaction caused by the buffer that empties in the incoming mainline I_1, as illustrated in Figure 11. Table 1 collects the values of the $\mathbf{L}^1$-error and of the order of convergence at time $T = 10$.
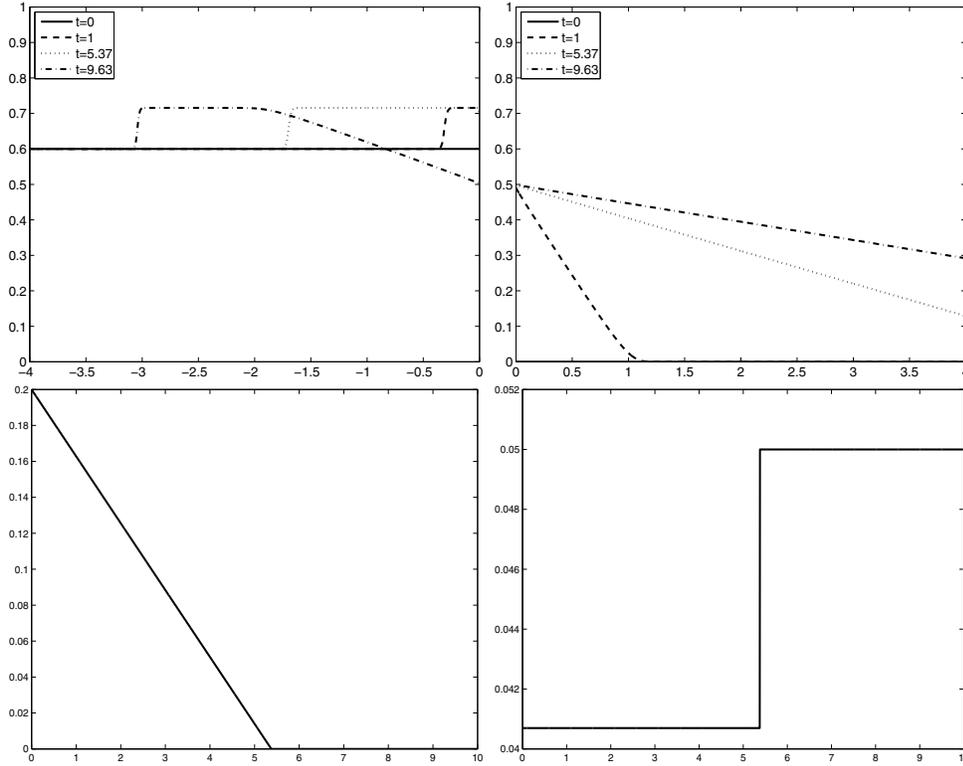
Fig. 11. *Evolution in time of the density in the incoming mainline (top, left) and on the outgoing mainline (top, right), and evolution of the flux in the onramp (bottom, left) and in the offramp (bottom, right), corresponding to initial data (5.4) and a space step discretization of $\Delta x = 0.01$.*

TABLE 1
Errors and order of convergence for the Godunov scheme at time $T = 10$, corresponding to initial data (5.4).

dx	$\mathbf{L^1}$-error	μ
0.02	$3.69 \cdot 10^{-2}$	0.8432
0.01	$1.49 \cdot 10^{-2}$	0.9133
0.005	$7.21 \cdot 10^{-3}$	0.9322
0.002	$1.10 \cdot 10^{-3}$	1.0962
0.001	$2.23 \cdot 10^{-4}$	1.2170

2. *Case* II: We consider the following initial data:

(5.5) $$\rho_1(0, x) = 0.1, \quad \rho_2(0, x) = 0.6.$$

In this case, the values of the initial conditions are chosen such that the wave produced by the buffer that empties can be seen in the outgoing mainline. In particular, in this case no waves are generated at the initial time. The only wave generated is a shock which appears once that the buffer empties at time $t = 1.53$, as shown in Figure 12. Table 2 reports the $\mathbf{L^1}$-error and the order of convergence.
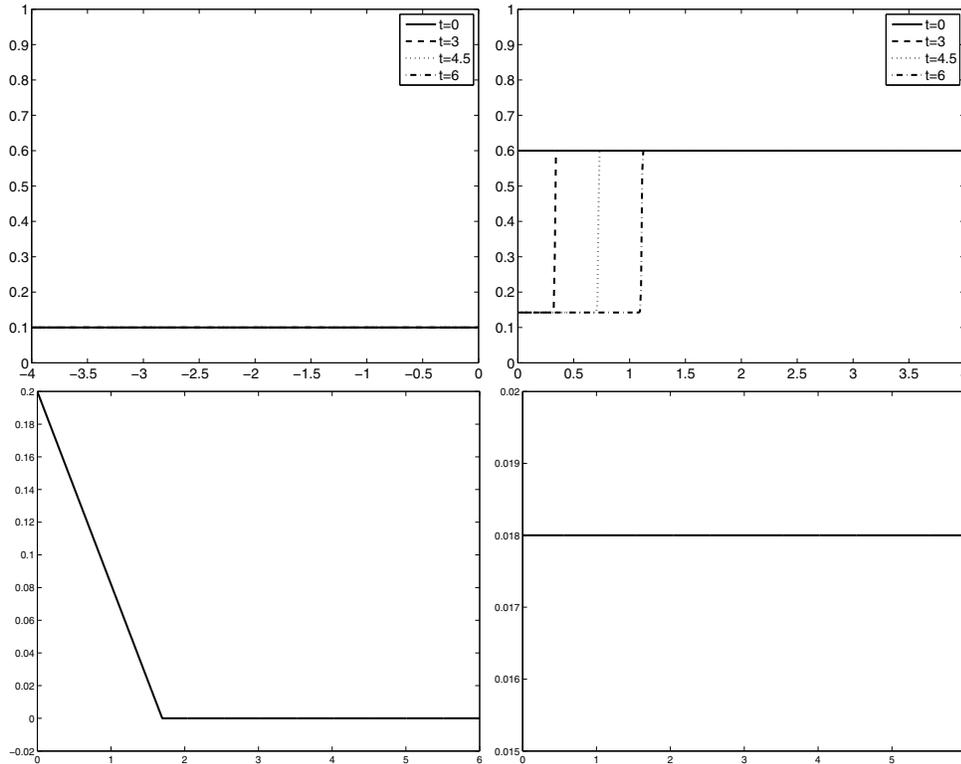
Fig. 12. *Evolution in time of the density in the incoming mainline (top, left) and on the outgoing mainline (top, right), and evolution of the flux in the onramp (bottom, left) and in the offramp (bottom, right), corresponding to initial data* (5.5) *and a space step discretization of* $\Delta x = 0.01$.

TABLE 2

Errors and order of convergence for the Godunov scheme at time $T = 3$, *corresponding to initial data* (5.5).

dx	$\mathbf{L^1}$-error	μ
0.02	$1.70 \cdot 10^{-2}$	1.0464
0.01	$1.67 \cdot 10^{-2}$	0.8890
0.005	$1.44 \cdot 10^{-2}$	0.8066
0.002	$9.39 \cdot 10^{-3}$	0.9878
0.001	$3.57 \cdot 10^{-4}$	1.2474

6. Conclusions. This article introduces a model of a 2×2 junction with an onramp and an offramp. The onramp is modeled by an ODE, which represents a vertical buffer. This way of handling boundary conditions makes it possible not to lose flow information. The junction flow distribution is solved through an *LP*-optimization problem, which maximizes the flow in the outgoing mainline. Moreover, a right-of-way parameter is introduced to ensure the uniqueness of the solution and a good representation of field experiences. The model is solved numerically using a modified Godunov scheme that takes into account the waves that can be produced when the buffer empties. Some numerical tests are presented to show the stability and

accuracy of the scheme. Moreover, from the analysis of the $\mathbf{L}^1$-error, the convergence of the scheme is demonstrated numerically.

REFERENCES

[1] C. Bardos, A. Y. le Roux, and J.-C. Nédélec, *First order quasilinear equations with boundary conditions*, Comm. Partial Differential Equations, 4 (1979), pp. 1017–1034.

[2] A. Bressan, *Hyperbolic Systems of Conservation Laws. The One-Dimensional Cauchy Problem*, Oxford Lecture Ser. Math. Appl. 20, Oxford University Press, Oxford, UK, 2000.

[3] G. Bretti, R. Natalini, and B. Piccoli, *Numerical approximations of a traffic flow model on networks*, Netw. Heterog. Media, 1 (2006), pp. 57–84.

[4] Y. Chitour and B. Piccoli, *Traffic circles and timing of traffic lights for cars flow*, Discrete Contin. Dyn. Syst. Ser. B, 5 (2005), pp. 599–630.

[5] G. M. Coclite, M. Garavello, and B. Piccoli, *Traffic flow on a road network*, SIAM J. Math. Anal., 36 (2005), pp. 1862–1886.

[6] R. M. Colombo, P. Goatin, and B. Piccoli, *Road network with phase transition*, J. Hyperbolic Differ. Equ., 7 (2010), pp. 85–106.

[7] A. Cutolo, B. Piccoli, and L. Rarità, *An upwind-Euler scheme for an ODE-PDE model of supply chains*, SIAM J. Sci. Comput., 33 (2011), pp. 1669–1688.

[8] C. M. Dafermos, *Hyperbolic Conservation Laws in Continuum Physics*, Springer, New York, 2009.

[9] M. Garavello and P. Goatin, *The Cauchy problem at a node with buffer*, Discrete Contin. Dyn. Syst. Ser. A, 32 (2012), pp. 1915–1938.

[10] M. Garavello and B. Piccoli, *Traffic flow on a road network using the Aw-Rascle model*, Comm. Partial Differential Equations, 31 (2006), pp. 243–275.

[11] M. Garavello and B. Piccoli, *Traffic Flow on Networks: Conservation Laws Model*, AIMS Ser. Appl. Math., American Institute of Mathematical Sciences, Springfield, MO, 2006.

[12] S. K. Godunov, *A finite difference method for the numerical computation of discontinuous solutions of the equations of fluid dynamics*, Mat. Sb., 47 (1959), pp. 271–290.

[13] S. Göttlich, M. Herty, and A. Klar, *Network models for supply chains*, Comm. Math. Sci., 3 (2005), pp. 545–559.

[14] M. Herty, A. Klar, and B. Piccoli, *Existence of solutions for supply chain models based on partial differential equations*, SIAM J. Math. Anal., 39 (2007), pp. 160–173.

[15] M. Herty, J. Lebacque, and S. Moutari, *A novel model for intersections of vehicular traffic flow*, Netw. Heterog. Media, 4 (2009), pp. 813–826.

[16] M. Herty, S. Moutari, and A. Rascle, *Optimization criteria for modelling intersections of vehicular traffic flow*, Netw. Heterog. Media, 1 (2006), pp. 275–294.

[17] W. Krichene, M. L. Delle Monache, J. Reilly, S. Samaranayake, P. Goatin, and A. M. Bayen, *A continuous model for traffic networks*, in preparation.

[18] S. N. Kružhkov, *First order quasilinear equations with several independent variables*, Mat. Sb. (N.S.), 81 (1970), pp. 228–255.

[19] P. Le Floch, *Explicit formula for scalar non-linear conservation laws with boundary condition*, Math. Methods Appl. Sci., 10 (1988), pp. 265–287.

[20] R. J. LeVeque, *Numerical Methods for Conservation Laws*, Lectures in Math. ETH Zürich, Birkhäuser, Cambridge, MA, 1992.

[21] R. J. LeVeque, *Finite Volume Methods for Hyperbolic Problems*, Cambridge Texts Appl. Math., Cambridge University Press, London, 2002.

[22] M. J. Lighthill and G. B. Whitham, *On kinematic waves. II. A theory of traffic flow on long crowded roads*, Proc. Roy. Soc. London Ser. A, 229 (1955), pp. 317–346.

[23] A. Muralidharan, G. Dervisoglu, and R. Horowitz, *Freeway traffic flow simulation using the link node cell transmission model*, in American Control Conference, 2009.

[24] A. Muralidharan and R. Horowitz, *Optimal control of freeway networks based on the link node cell transmission model*, in American Control Conference (ACC), 2012, pp. 5769–5774.

[25] P. I. Richards, *Shock waves on the highway*, Oper. Res., 4 (1956), pp. 42–51.

[26] I. S. Strub and A. Bayen, *Weak formulation of boundary conditions for scalar conservation laws: An application to highway traffic modelling*, Internat. J. Robust Nonlinear Control, 16 (2006), pp. 733–748.

[27] D. Work, S. Blandin, O.-P. Tossavainen, B. Piccoli, and A. M. Bayen, *A distributed highway velocity model for traffic state reconstruction*, Appl. Math. Res. Xpress. AMRX, 1 (2010), pp. 1–35.